The Feedback between Equatorial Convection and Local Radiative and Evaporative Processes: The Implications for Intraseasonal Oscillations

MARIA FLATAU AND PIOTR J. FLATAU

Scripps Institution of Oceanography, University of California, San Diego, La Jolla, California

PATRICIA PHOEBUS

Naval Research Laboratory, Monterey, California

PEARN P. NIILER

Scripps Institution of Oceanography, University of California, San Diego, La Jolla, California

(Manuscript received 10 August 1995, in final form 27 March 1997)

ABSTRACT

Existing theories of the Madden–Julian oscillation neglect the feedback between the modification of sea surface temperature by the convection and development of a convective cluster itself. The authors show that the convection-generated SST gradient plays an important role in cluster propagation and development. The relative importance of radiative and evaporative fluxes in SST regulation is also discussed. Various Tropical Ocean Global Atmosphere Coupled Ocean–Atmosphere Response Experiment and Central Equatorial Pacific Experiment observation platforms are used to estimate the effects of equatorial convection on SST changes during March 1993. The data include drifting buoys and TAO-buoy array measurements, combined with the Navy Operational Global Atmospheric Prediction System analyzed surface wind fields and Geostationary Meteorological Satellite cloud-top temperatures. It is shown that during the equatorial convection episode SST is decreasing under and to the west of the convective heat source due to the large wind velocities and solar flux reduction. To the east of the source, in the convergence region of a Kelvin wave, low wind speeds and high insolation cause the SST to increase.

The data are used to formulate an empirical relationship between wind speed and the 24-h SST change on the equator. Although formulated in terms of wind speed, this relationship implicitly includes radiative effects. This equation is then used in a global circulation model to examine the effect of SST feedback on the behavior of equatorial convection. A series of experiments is performed using an R15 general circulation model of the ''aquaplanet'' with a zonally symmetric SST distribution. In the case with fixed SSTs, equatorial wind fluctuations have the character of waves propagating around the globe with a phase speed of about 20 m s^{-1}. When the effect of SST modification is included, the fluctuations slow down and become more organized. In addition, a 40–60-day peak appears in the spectral analysis of equatorial precipitation.

1. Introduction

The purpose of this paper is to understand the mutual interaction of equatorial convection and SST on the intraseasonal timescale. The most pronounced signal in the equatorial convection is connected with the 40–50 day oscillations, frequently called Madden–Julian oscillations (MJO), described first by Madden and Julian (1971) as global-scale eastward propagating zonal circulation cells along the equator. This type of oscillation is usually connected with the zonal wave 1–2 circulation anomalies and corresponding convection anomalies. Wind anomalies have characteristics of the first baroclinic mode, with the low-level wind out of phase with the upper-level wind. Convection anomalies are confined to the Indian Ocean and Western Pacific warm pool regions, while wind perturbations tend to propagate around the equator. In addition to the eastward movement of the system, individual cloud clusters propagate westward (Nakazawa 1988). The eastward propagation of this phenomenon was initially explained as the manifestation of convectively driven, equatorially trapped Kelvin modes. In this theory, the convergent phase of the Kelvin wave triggers the convection, which in turn maintains and slows the propagating wave (wave-CISK mechanism). However, the classic wave-CISK theory predicts wave speeds faster than the observed propagation speed of the intraseasonal oscillation. A number

Corresponding author address: Dr. Piotr J. Flatau, Scripps Institution of Oceanography, California Space Institute, University of California, San Diego, 8605 La Jolla Shores Drive, La Jolla, CA 92093-0221.
E-mail: pflatau@atol.ucsd.edu

of theories were offered to explain the slowdown of the propagating wave-CISK modes, for example, damping of the waves (Chang 1977) or positive-only heating (Lau and Peng 1987). Lau et al. (1989) contains an elegant explanation of the eastward propagation of super cloud clusters and westward motion of individual clusters. Using a global model whose convective parameterization was based on the wave-CISK mechanism, they show that westward propagating, high-frequency modes are a manifestation of Rossby waves, while slow eastward motion of the whole system is driven by the formation of new convective centers in the convergent regions of a Kelvin wave. Existing theories of MJO development and propagation (Lau et al. 1989; Emanuel 1987; Neelin et al. 1987; Hu and Randall 1994) concentrate on atmospheric processes and neglect the feedback between SST modification by convection and the development of a cluster itself. Even air–sea interaction theories (Emanuel 1987; Neelin et al. 1987) consider the effect of evaporative fluxes on the atmospheric boundary layer without taking into account the effect of the fluxes on SST. In some of their experiments, Neelin et al. (1987) include the effect of SST change in the form of the ''swamp'' boundary condition. However, because of the lack of vertical mixing processes and drastic simplifications of radiation (clouds prescribed as a function of latitude), the simulated SST changes are not likely to be realistic, and therefore their feedback on development of eastward propagating modes cannot be properly assessed.

Some facts, however, indicate that such a feedback can influence the development of equatorial superclusters. First, the significance of SST changes generated by a convective system has been shown for other tropical systems, such as tropical cyclones (Khain and Ginis 1991). Using a coupled ocean–atmosphere model, they showed that cyclone-induced SST changes drastically influence the distribution of convection in the storm, with convection concentrated in sectors with the warmest SST. This distribution of convection influences the motion of the system, which moves away from the low SST ''wake.'' Second, as shown by Li and Wang (1994), on the seasonal timescale the SST distribution plays an important role in variations of the MJO. Finally, recent observations [e.g., Tropical Oceans Global Atmosphere Coupled Ocean–Atmosphere Response Experiment (TOGA COARE)] emphasize the role of surface fluxes related to convection in modifying SST in the western equatorial Pacific. For example, westerly wind bursts associated with the convective phase of the MJO, observed during the TOGA COARE Intensive Observation Period, caused an SST drop of over 1°C, with profound changes in the oceanic mixed layer structure (Webster 1994). As shown by Bi (1995), the effect of surface fluxes during the IOP burst was strong enough to reverse the SST zonal gradient in the Western Pacific, with the temperature increasing toward the east.

In this paper, various TOGA COARE and Central Equatorial Pacific Experiment (CEPEX) observation platforms are used to estimate the effects of equatorial convection on SST changes during March 1993. The data include drifting buoys and Tropical Atmosphere Ocean (TAO) measurements, Navy Operational Global Atmospheric Prediction System (NOGAPS) analyzed surface wind fields, and Geostationary Meteorological Satellite (GMS) cloud-top temperatures. Using these data we develop the conceptual model of a convection–SST feedback on the intraseasonal timescale (Flatau and Flatau 1996). We also derive a simple empirical relationship between SST change and zonal wind on the equator. This relationship is then used in a general circulation model to study the effect of the SST–convection feedback on the development of equatorial convection.

2. Observational analysis of the convectively driven SST modification in the Western Pacific

a. Data

The data used in this section come from various sources. We concentrate our analysis on March 1993 when the CEPEX was conducted in the tropical Pacific. The data collected during this experiment are used in this paper. In addition, many TOGA-COARE-related platforms supplied data. Lagrangian drifting buoys released in the Western Pacific in February and March 1993 as part of TOGA COARE effort (Ralph et al. 1997) are used to obtain SST and oceanic surface currents in the equatorial region of the Western Pacific. The sea temperatures are measured by a thermistor on a surface float, 10 cm below the surface. The buoy's drogue is centered at 15 m. In most of the calculations we are using buoys located within 3 degrees of the equator, between 150°E and the date line. The position of the drifting buoys, SST and ocean current measurements were available every 6 hours. TAO ATLAS buoys were used to look at surface winds and the temperature structure of the mixed layer in the vicinity of the drifting buoys.

Atmospheric data were also gathered from a variety of sources. The cloud-top temperatures and albedo were obtained from GMS data converted to a 0.5° grid. To assess the synoptic situation in the area of interest, we used the analyzed fields from NOGAPS, a system that has been shown to have considerable skill in the tropical Pacific (Goerss and Jeffries 1994; Kindle and Phoebus 1995). NOGAPS consists of a multivariate optimum interpolation analysis (Goerss and Phoebus 1992), a nonlinear normal mode initialization, and a global spectral forecast model (Hogan and Rosmond 1991). For this study, NOGAPS was executed using a T79 version of the global spectral model, which has a physical grid resolution of approximately 1.5°. The NOGAPS surface wind is valid at 10 m, and surface wind speed observations from the SSM/I are routinely assimilated into

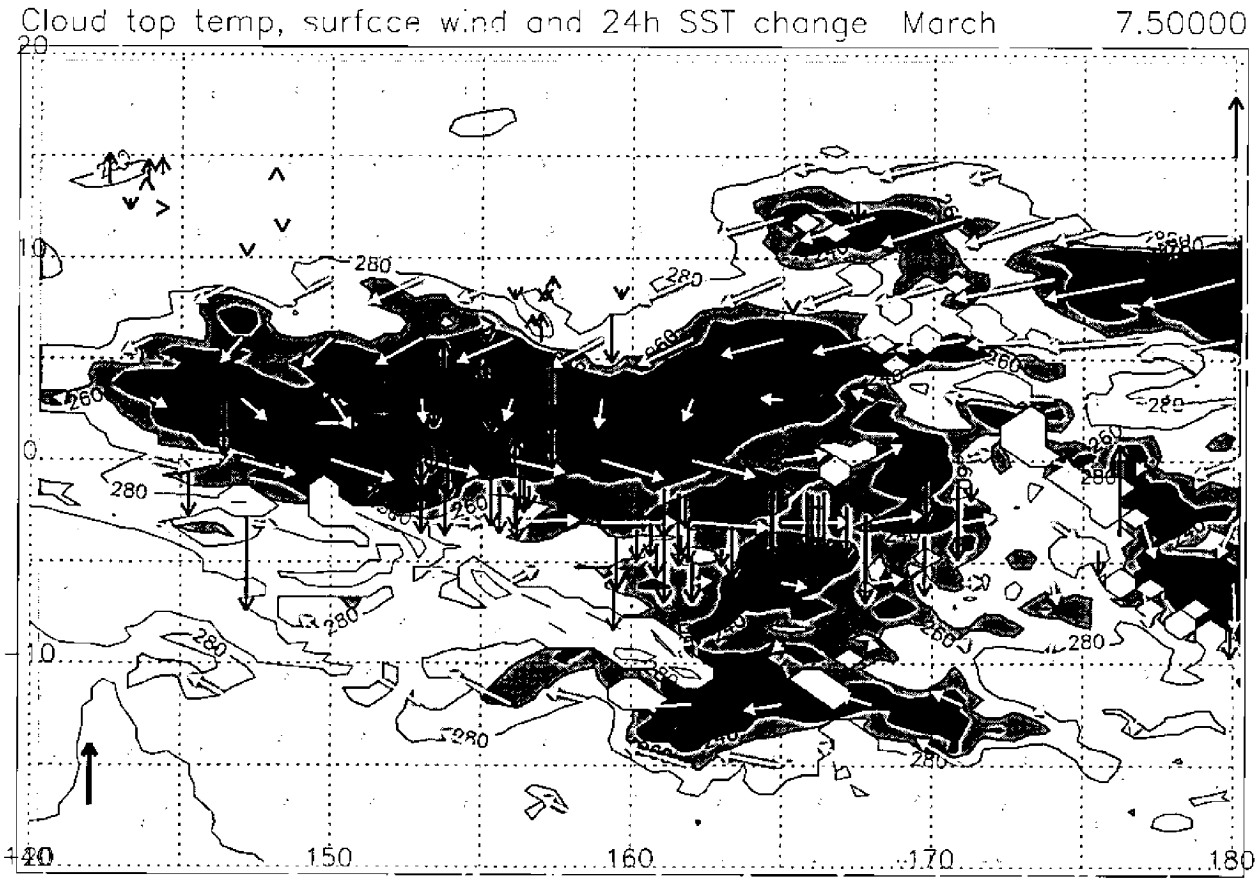

FIG. 1. NOGAPS surface (10 m) winds (white arrows), GMS cloud-top temperatures (shaded, in K), and drifters 24-h SST change (black arrows) on 7 March 1993. The scale in lower-left corner shows wind speed of 10 m s^{-1} and 0.1° day^{-1} SST change.

this system, a particularly attractive feature for our purposes.

To examine the relationship between wind fields, cloudiness, surface currents, and SST the NOGAPS surface (10 m) winds and the GMS data are interpolated to the drifting buoy positions.

b. The influence of equatorial convection on SST changes during March 1993

During our analysis period (March 1993) two episodes of equatorial convection were observed. The first began on 5 March, in the vicinity of the local SST maximum at 170°E, and ended in the formation of twin tropical cyclones Irma and Roger on 13 March 1993. The second episode developed on 18 March near 165°E and lasted for 3 days. In agreement with Gill's (1980) arguments on the circulation response to an equatorial heat source, both of these episodes were associated with westerly wind anomalies on the equator, with the maximum surface westerlies reaching 10 m s^{-1} in the case of the 5 March episode, but only 5 m s^{-1} for the late March event.

The wind and cloud-top temperatures, along with the 24-h SST changes observed during the stronger March event, are shown in Figs. 1 and 2. Initially (Fig. 1) the convective activity was concentrated on the equator. A narrow strip of strong westerly winds developed below the convective heat source, while to the east of the heat source weak easterlies prevailed. During this stage, the SSTs decreased in the region of westerly winds. As can be seen in Fig. 1, both large surface fluxes related to strong westerly winds and the presence of high clouds with their large albedos could contribute to the observed SST drop. Even though we have less drifter data in the convergence zone between easterly and westerly winds, the existing buoys indicate either no significant change or an increase of SST in this region.

Figure 2 depicts the situation on 13 March 1993, right after the tropical depressions on both sides of the equator reached tropical cyclone strength (Irma at 5.9°N, 160°E and Roger at 13°S, 165°E). Even though the equatorial winds remained strong west of 160°E, the convection shifted off the equator and became centered in developing storms. The SST began to rise—especially in the region of the low-level divergence between the storms. Near the center of Irma, a SST drop can be observed. As the storms moved poleward and westward, the equa-

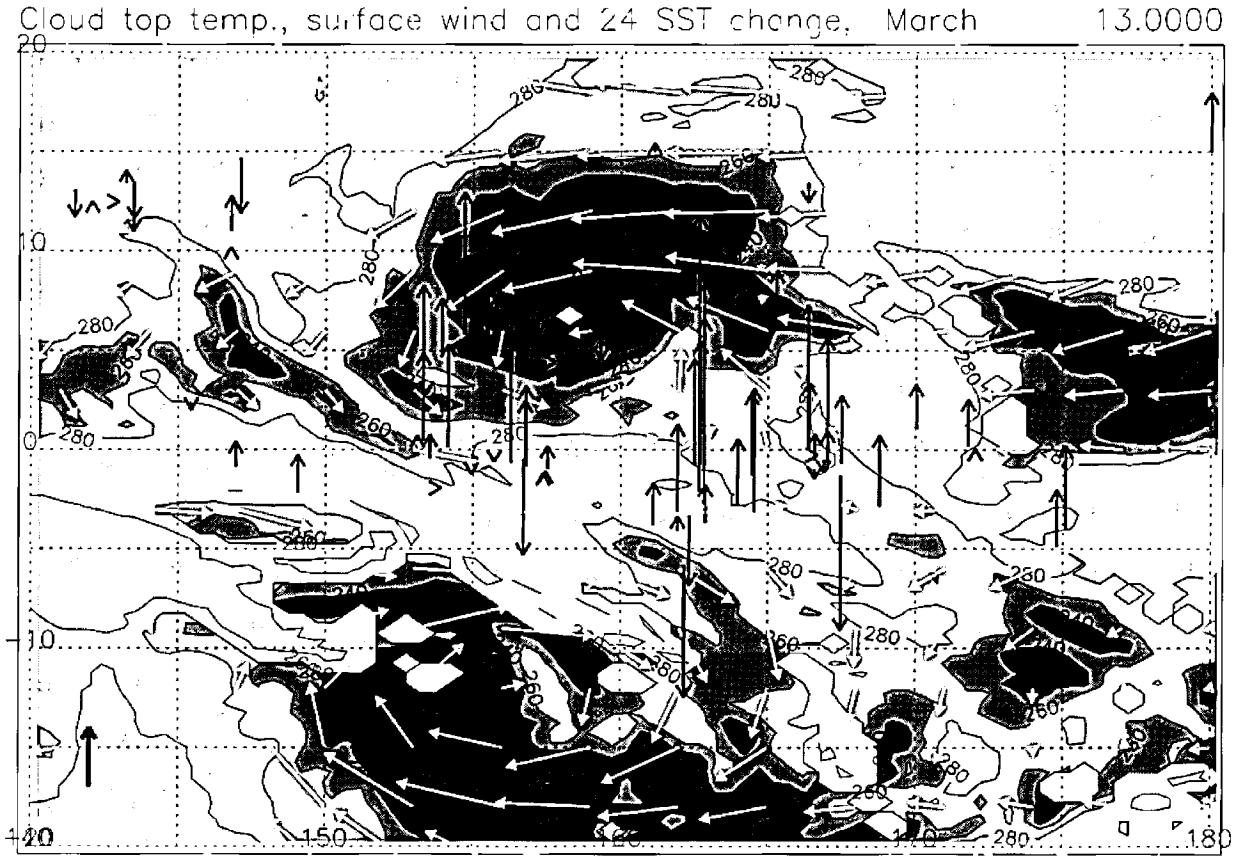

FIG. 2. NOGAPS surface (10 m) winds (white arrows), GMS cloud-top temperatures (shaded, in K), and drifters 24-h SST change (black arrows) on 13 March 1993. The scale in lower-left corner shows wind speed of 10 m s^{-1} and 0.1° day^{-1} SST change.

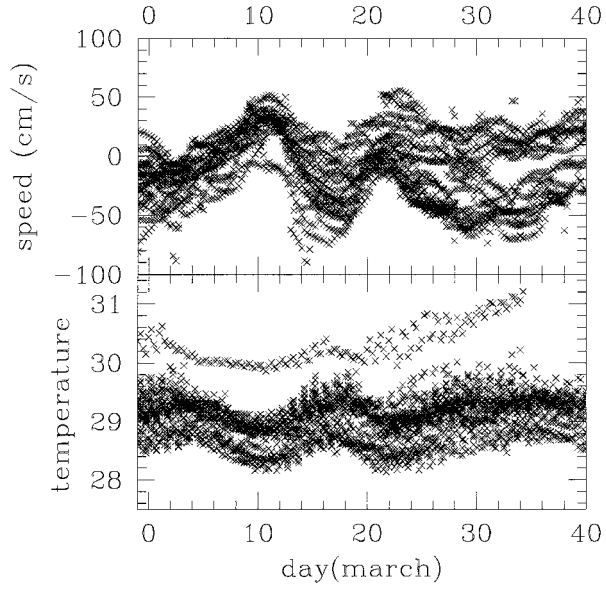

FIG. 3. Surface (15 m) currents and SST measured by Lagrangian drifters during March 1993. The buoys locations are between 3°S and 3°N, 150°E and the date line.

torial westerly winds propagated westward and weakened and the equatorial SST continued to rise.

The response of equatorial surface currents and SSTs to the March 1993 atmospheric events, as measured by drifting buoys, is shown in Fig. 3. The increase in equatorial westerlies was followed by a change in the direction of the ocean equatorial surface current. A comparison of the current velocities measured by each buoy with the wind speeds interpolated to the buoy's location showed that the lag in response was about 5 days. The eastward acceleration of the drifters was accompanied by a SST decrease, while for the westward moving buoys the temperatures generally increased. This behavior can be explained in two ways.

First, since the magnitude of the westerlies associated with the equatorial convection is usually larger then the magnitude of the easterly winds developing east of the heat source, evaporative fluxes are larger during westerly wind episodes. The analysis of evaporative fluxes from TAO buoys as well as from NOGAPS model field data shows that this was indeed the case, especially during the early March westerly burst. In NOGAPS, the

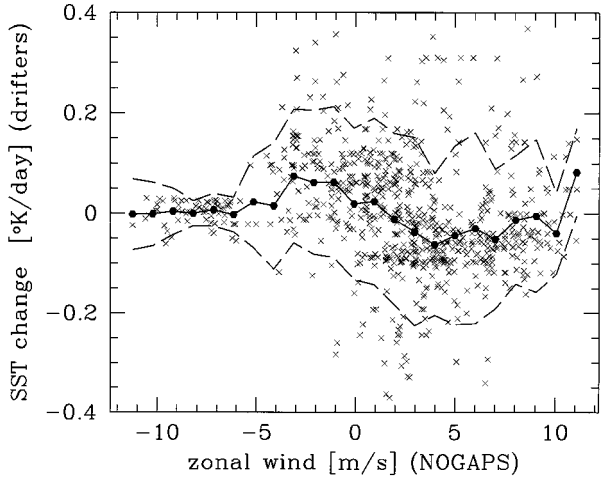

FIG. 4. The 24-h change of SST measured by drifters as a function of the surface wind at the buoy location. The solid line represents the average for $u + \Delta u$ to $u - \Delta u$ where $\Delta u = 0.5$ m s^{-1}, the dashed line the average plus/minus one standard deviation.

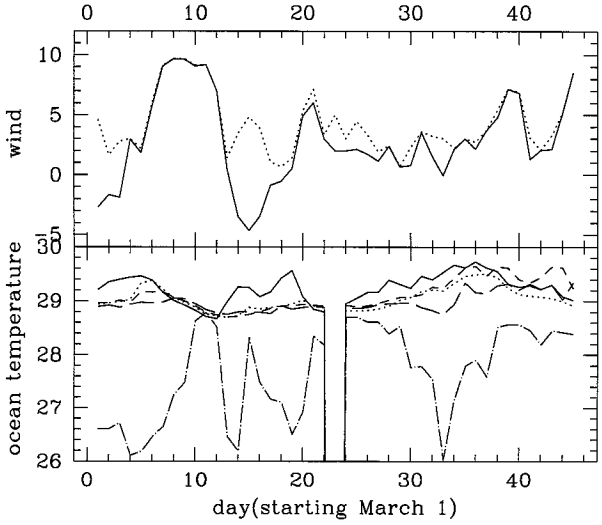

FIG. 6. Wind and ocean temperature at 2s165e ATLAS buoy. Upper panel: zonal wind velocity (solid line), total wind speed (short dashed line); lower panel: SST (solid line), 25-m (short dashed), 50-m (medium dashed) 75-m (long dashed), and 100-m (dot–dashed) temperatures.

surface latent flux on the equator near 160°E reached 200 W m^{-2} during the burst, compared to about 80 W m^{-2} after the cyclones moved poleward. Similarly, the evaporation calculated by bulk formula from the TAO buoy data indicates that for sea surface temperatures of about 29°C the largest fluxes (200 W m^{-2}) were associated with the strongest westerlies (10 m s^{-1}), while easterlies in this region seldom exceed 5 m s^{-1} and had associated evaporative fluxes of about 100 W m^{-2} or less.

Another explanation involves reduction of the solar flux by convective clouds associated with the diabatic heat source, emphasized by Ramanathan and Collins (1991). To look closer at how these two mechanisms contribute to the SST changes observed by drifting buoys, we calculate the average 24-h SST change as a function of the zonal wind velocity from NOGAPS analyses and the GMS cloud-top temperatures T_B collocated with the position of the buoys. Since SST time derivatives are calculated following Lagrangian drifters, they reflect vertical fluxes at the position of the drifter.

Figure 4 shows the 24-h SST change as a function of zonal wind, for drifting buoys located within 3° of the equator. The solid line shows the SST change averaged for zonal winds from $u + \Delta u$ to $u - \Delta u$, where $\Delta u = 0.5$ m s^{-1}.

As can be expected from evaporative fluxes, the largest heating occurs for small zonal wind velocities. However, there is a significant asymmetry in SST change between easterly and westerly winds, which cannot be

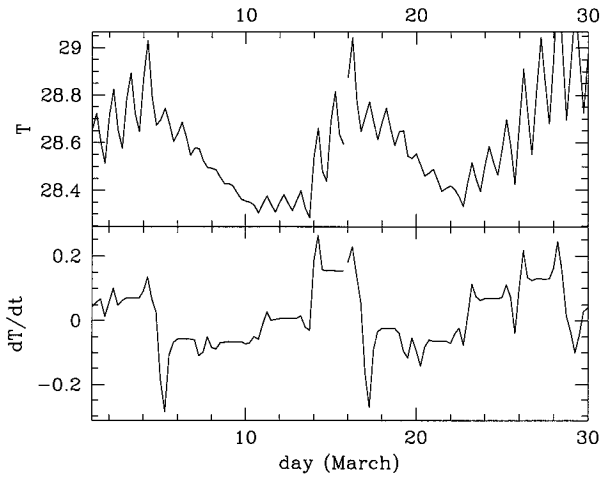

FIG. 5. The sea surface temperature and 24-h SST change following the buoy 15561 (near 0.6°S, 165°E).

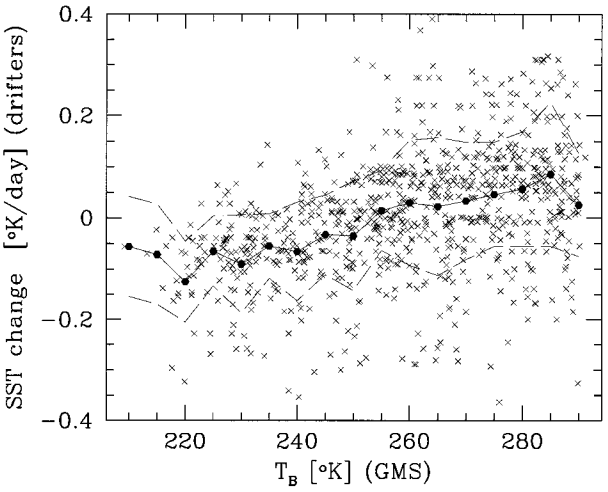

FIG. 7. Twenty-four-hour SST change as a function of cloud-top temperature T_B (GMS).

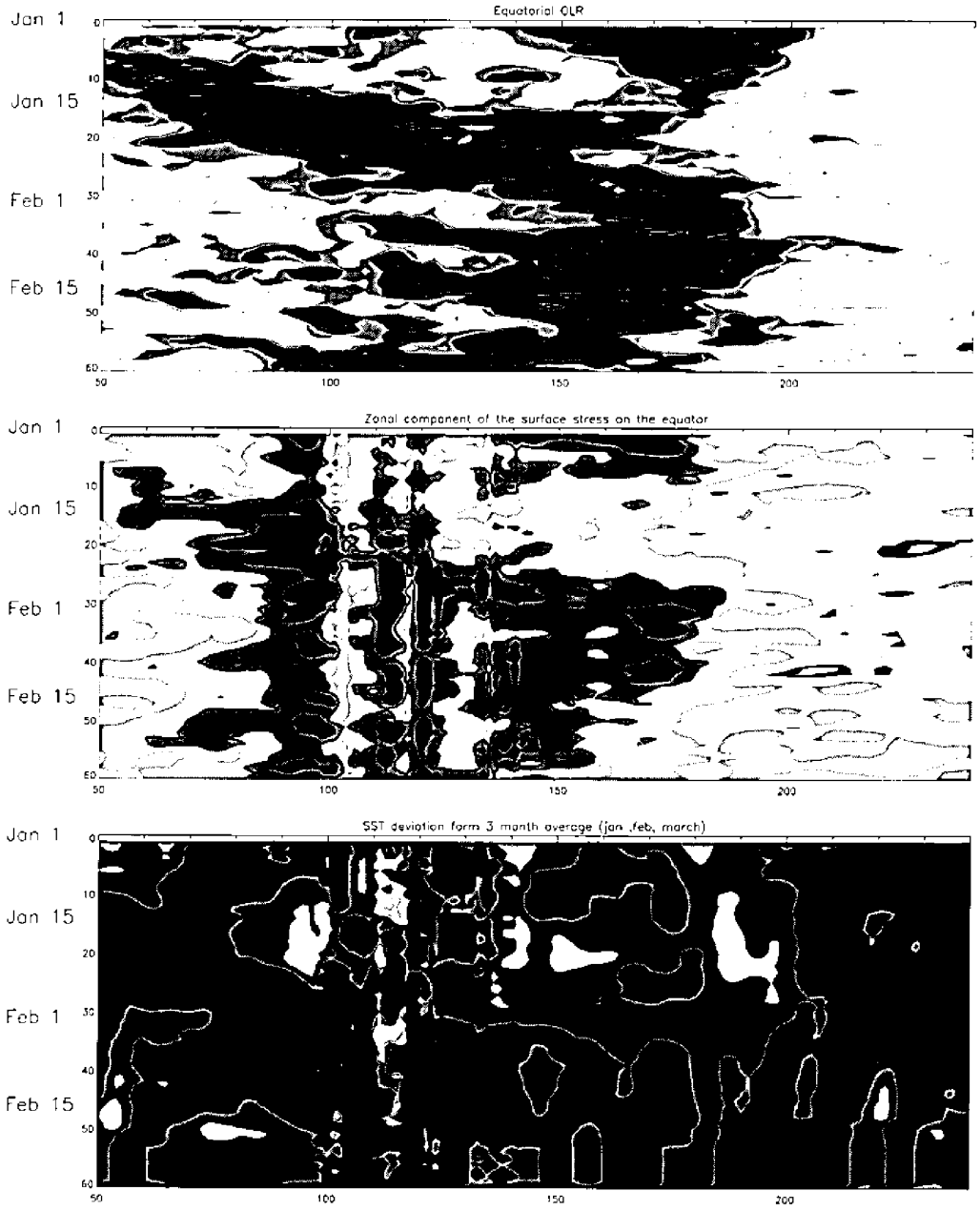

FIG. 8. Time–longitude diagram of cloud-top temperatures, zonal component of the wind stress, and deviation of SST from the January–March average during the passage of ISO episode. Dark shading denotes high cloud tops, negative zonal wind stress, and negative deviation of SST. SST contours are marked every 0.4°C.

explained by the effects of evaporation alone. While the averaged SST change is positive for all easterly winds, with the maximum at $u = -3$ m s^{-1}, cooling dominates for westerlies stronger than 2 m s^{-1}. The average SST change for easterlies decreases with the magnitude of the wind velocity. This relationship can be explained by the increasing role of the evaporative cooling competing with the clear-sky solar fluxes.

The large scatter of the data can be explained by combined effects of various surface fluxes and changing depth of the mixed layer. The influence of the mixed layer depth on the magnitude of the SST change for March 1993 convective events is illustrated in Figs. 5 and 6, representing the temperature and the 24-h change of SST for one of the drifting buoys, and wind and ocean temperatures at the TAO ATLAS (Autonomous Temperature Line Acquisition System) buoy located near the drifter. Since only temperature data are available, the mixed layer in this case is defined by temperature profiles. The density mixed layer can be quite different

because of the salinity effects and presence of the ''barrier layer.'' Comparison of Figs. 5 and 6 suggests that very large SST tendencies were associated with a shallow mixed layer in the ocean. For example, at the beginning of the westerly burst (5 March) the SST drop was sudden and, as wind magnitude was still relatively small, the temperature decrease was probably related to the reduction of the solar flux. Figure 6 indicates that the initial large SST drop was confined to a very shallow layer. As the mixed layer depth increased with growing wind speed, the effect of surface fluxes was spread over the deeper layer and SST changes were smaller. After the convection moved off the equator (after 12 March), the increasing solar fluxes began to heat and stabilize the surface layer, even though the equatorial westerlies were still relatively strong. When the equatorial winds weakened, the SST rapidly increased. The high SSTs provided favorable conditions for the development of convection, and on 18 March the SST again rapidly decreased.

The relationship between SST change and GMS-derived cloud-top temperature is more straightforward. In Fig. 7 we show the average 24-h change of SST as a function of cloud-top temperatures T_B averaged over six hours. Although there is large scatter in the data, the average SST change is positive for T_B greater than 255 K and negative for colder cloud tops. This relationship corresponds well with the linear relationship between T_B and net cloud effect on surface forcing observed in CEPEX (Collins et al. 1996). As shown by Collins et al. (1996), on the surface, the ''shading'' effect is greater than longwave heating, and the net radiative effect of clouds is to cool the surface. The dependence between the net cloud surface forcing $C_{\text{net}}(0)$ and cloud-top temperatures T_B can be approximated by a linear relation, $C_{\text{net}}(0) = 2.8 - (290 - T_B) - 7$.

The contribution of the radiative effects to SST changes can be roughly estimated by comparing 24-h SST changes for -3 m s^{-1} easterlies (corresponding to the maximum temperature increase) to those for 3 m s^{-1} westerlies. We chose the identical wind speed for our comparisons to minimize the influence of evaporative fluxes and mixing effects on SST tendency. Therefore the difference may be attributed to radiative effects of the convective clouds in the westerlies region. We calculate the net flux F_n as

$$F_n = \frac{d\text{SST}}{dt}\rho_w d_m L_w,$$

where dSST/dt is the SST change estimated from drifters, ρ_w and L_w are the density and specific heat of water, and d_m is the depth of mixed layer. We use a 4-m mixed layer depth for the undisturbed period (characterized by easterly winds) and a 23-m mixed layer depth for the disturbed period (westerly winds). These values are based on Webster et al. (1996) calculations of SST and mixed layer properties for different atmospheric conditions. Their results were obtained using TOGA COARE IOP measurements supplemented with a one-dimensional model of the oceanic mixed layer. If the values for the whole month of March 1993 are used, the average dSST/dt is 5.6×10^{-2} K day^{-1} for $u = -3$ m s^{-1} and -2.7×10^{-2} K day^{-1} for $u = 3$ m s^{-1}, which gives the average net vertical flux of 11.6 W m^{-2} under easterlies and -26 W m^{-2} under westerlies. Therefore the difference in net surface fluxes between disturbed and undisturbed conditions, with the same average wind speeds of 3 m s^{-1} is about 38 W m^{-2}. If only the data from the stronger episode (1–15 March) are considered, the net flux difference becomes 50 W m^{-2}, due to the fact that the equatorial radiative fluxes were unusually large right after formation of the twin cyclones.

3. Modification of equatorial convection by SST feedback—Numerical results

a. Conceptual model of convection–SST feedback

The observational results presented in the previous section suggest a strong influence of equatorial convective systems on local changes of underlying sea surface temperature. These results agree with other TOGA COARE observations of the decrease in SST and heat content during MJO-related westerly bursts (Webster 1994) and the coincidence of highest SST with weakest winds (Serra et al. 1997). Figure 8 illustrates the relationships between equatorial cloud-top temperatures, zonal wind stress, and SST during MJO episodes observed during TOGA COARE IOP (from ECMWF analysis). The presence of high clouds is associated with westerly surface winds. The sea surface temperatures are highest before the onset of convective activity and drop sharply after MJO passage.

Nakazawa's (1995) detailed analysis of intraseasonal oscillation (ISO) episodes observed during the TOGA-COARE IOP showed that high SST preceeded convective activity by 12–13 days. In addition maximum total precipitable water observed by SSM/I was leading convection by about 5–10 days. In the case of IOP convective systems, the increase in precipitable water occured in the regions of relatively small winds and therefore could not be attributed to wind-evaporation feedback. Nakazawa suggests that this moisture increase was related to enhanced evaporation associated with moisture deficit terms in regions of high SST.

Based on our observations and results from TOGA COARE we suggest a new conceptual model of intraseasonal oscillation, taking into account the interaction between SST and equatorial convection. We call it air–sea convective intraseasonal interaction (ASCII). A comparison of ASCII with the wave-CISK theory of intraseasonal oscillation (Lau et al. 1989) and the wind-induced surface heat exchange theory (Emanuel 1987) is shown in Fig. 9.

In the wave-CISK theory the region of convergence

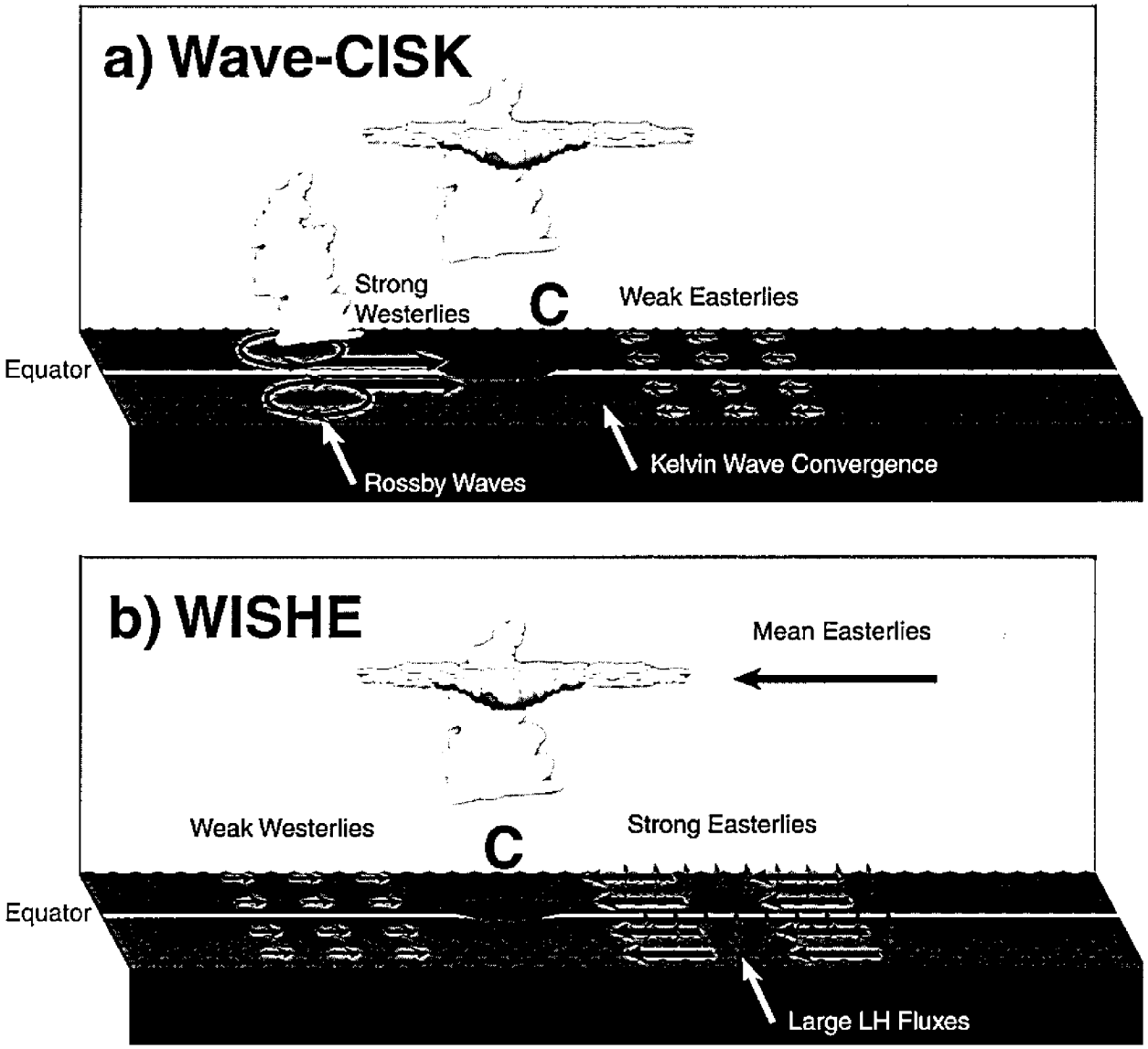

FIG. 9. The illustration of three conceptual models of intraseasonal oscillation. (a) Wave-CISK, (b) wind-induced surface heat exchange (WISHE), and (c) air–sea convective intraseasonal interaction (ASCII).

between easterlies and westerlies in an eastward propagating Kelvin wave (region C in Fig. 9) becomes the preferred site for the subsequent development of convection. The formation of the new cells in this region causes the eastward propagation of the equatorial supercluster, while the individual clusters that form on both sides of the equator move west as Rossby waves (Lau et al. 1989) This approach was criticized by Emanuel (1987), who argued that convection does not create atmospheric temperature perturbation but only redistributes the boundary layer Θ_e. Therefore, if convection is caused solely by convergence of moisture at constant Θ_e, adiabatic cooling exactly balances diabatic heating and there is no temperature perturbation in the troposphere and development of growing, eastward propagating modes is not possible. Recent numerical models of tropical wave instabilities (Brown and Bretherton 1995; Yu and Neelin 1994) indicate that earlier successes in modeling of MJO as wave-CISK instability depended on the use of Kuo-like parameterization that explicitely includes the relationship between convergence and development of convection. When other parameterizations of convection like convective adjustment scheme (Yu and Neelin 1994) or Emanuel parameterization (Brown and Bretherton 1995) are used, wave-CISK modes do not develop.

Emanuel (1987) as well as Neelin et al. (1987) argued that, in the presence of the mean equatorial easterly wind, enhanced surface evaporation in the region of the strong easterlies (Fig. 9b) can provide surface forcing

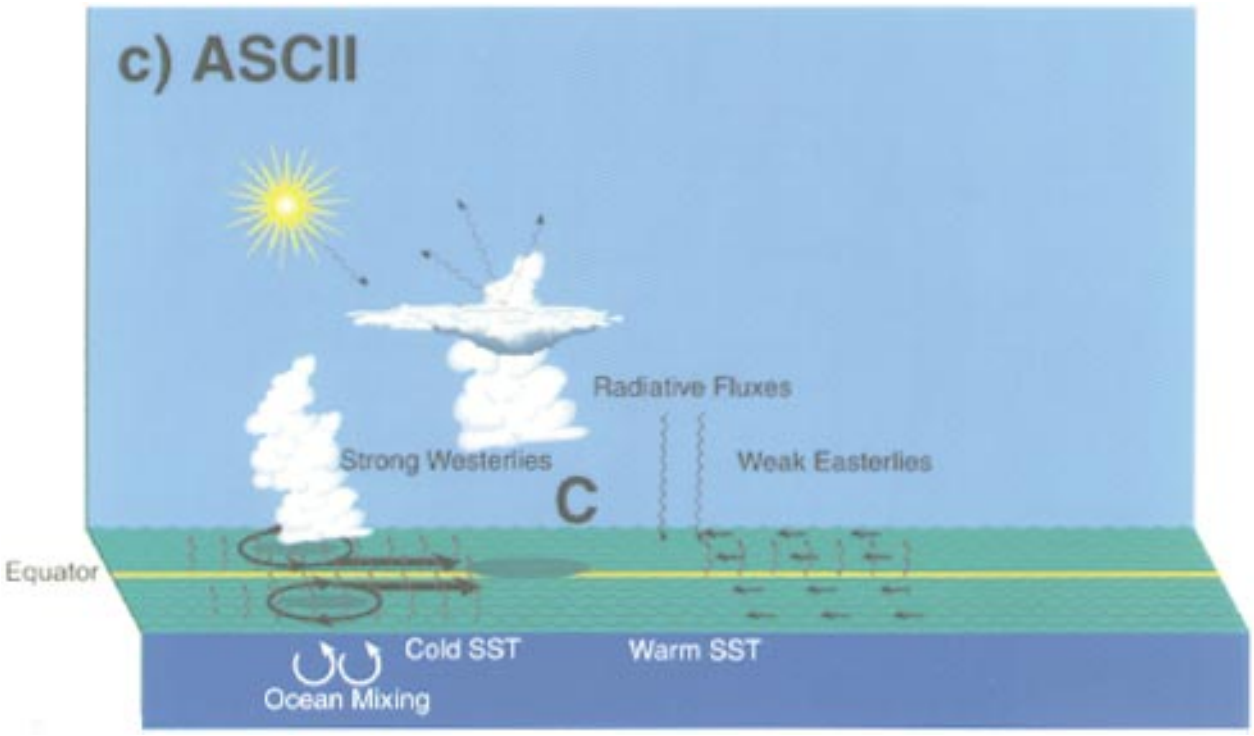

FIG. 9. (*Continued*)

necessary for development of instabilities similar of observed oscillations. This process is usually referred to as wind-induced surface heat exchange (WISHE). Increased surface fluxes in the region of large easterlies are responsible for positive temperature perturbations that cause the eastward propagation of the wave and provide energy for growth of instability. However, the results from the TOGA-COARE IOP (Lin and Johnson 1996) suggest that, contrary to the behavior postulated by Emanuel (1987) or Neelin, in the warm pool region the maximum surface fluxes associated with the presence of strong winds tend to develop underneath and toward the west of the convective system, since equatorial westerlies (''westerly bursts'') are usually stronger than easterlies (Gill 1980). In addition, the assumption of mean easterly flow used by Emanuel and Neelin is not always true, especially during the El Niño years.

In our hypothesis (Fig. 9c) the surface forcing necessary for enhancement of the Kelvin wave is provided by the SST distribution generated by the supercluster itself. As we have shown in the previous section, in a narrow band of strong westerlies underneath the cluster, SST drops not only due to evaporation but also because of oceanic vertical mixing and cloud shielding effects. However, east of the convective source, in the region of the weak easterly winds, the conditions exist for increase in SST (Serra et al. 1997; Nakazawa 1995). This configuration favors the increase of the surface moist entropy east of the system and development of convection in the convergent region of the Kelvin wave.

Both our theory and WISHE emphasize the importance of surface fluxes in maintaining the convection. However, if the ocean is treated as an infinite energy source, the increased wind speed is necessary for raising the surface moist static energy east of a convective complex. If the ocean is allowed to respond to convection, the surface forcing related to SST changes can provide surface moist static energy anomalies, necessary for growth and propagation of eastward propagating perturbations. When the modification of SST by convective systems is allowed, the regions of weak surface winds—rather than strong winds—become the preferred sites for future convective development.

b. Model results

We examine the influence of local, convectively generated SST changes on the development of equatorial convection in a general circulation model with wind-dependent equatorial SST. The numerical model we use here is a modified version of the Lau et al. (1989) R15 spectral model. Instead of a Kuo-like convective parameterization, which explicitly ties the convection to the low-level convergence, and therefore favors the wave-CISK mechanism, the Emanuel (1991) scheme, based on CAPE, is used. All the experiments described in this

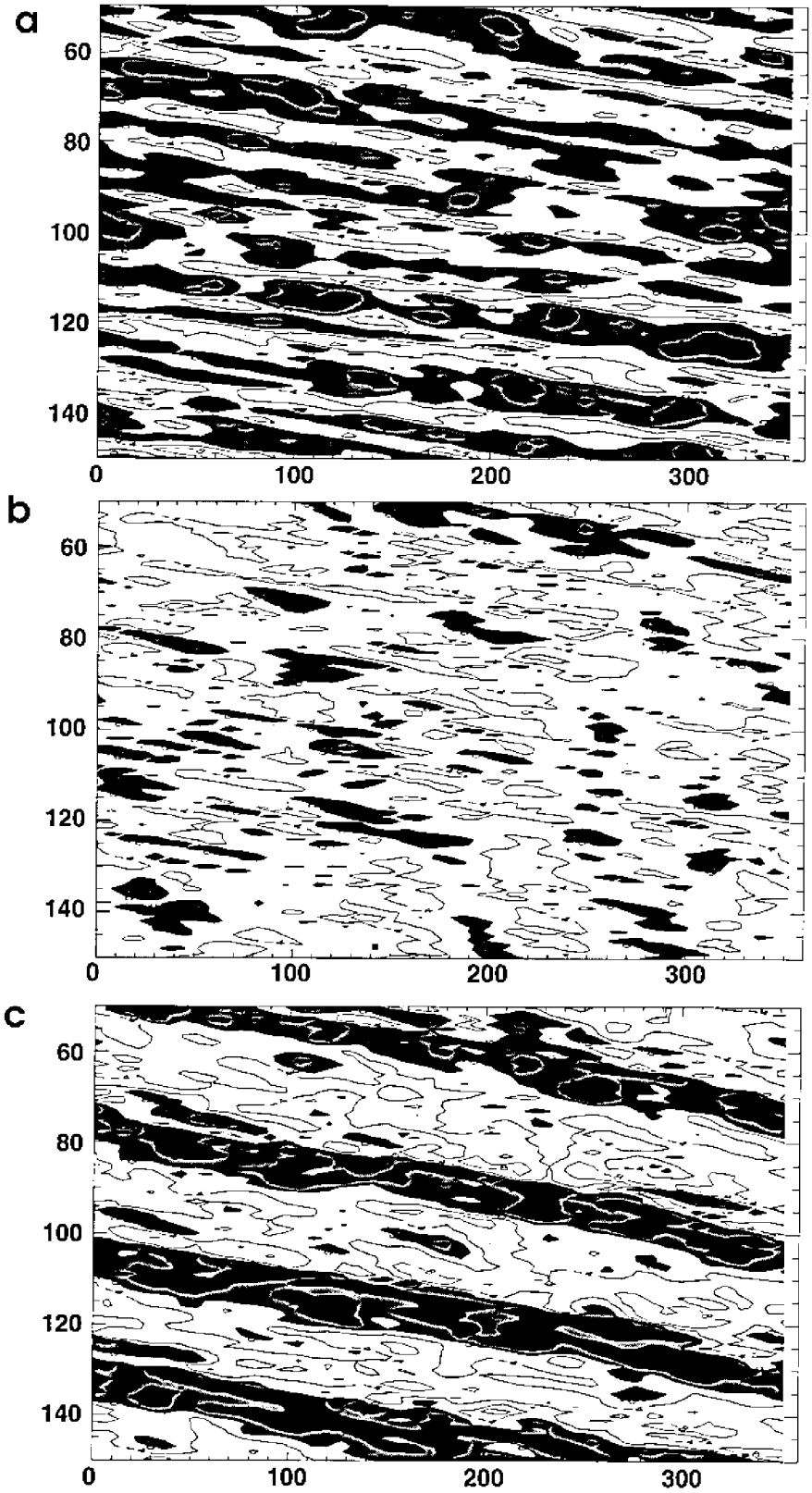

FIG. 10. Longitude–time (in days) diagram of the equatorial winds for (a) constant SST, (b) constant SST and wind–evaporation feedback removed, and (c) equatorial SST modified.

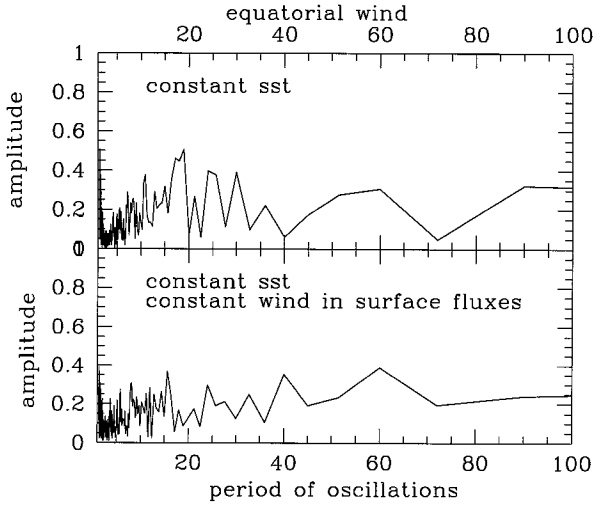

FIG. 11. Spectral analysis of equatorial wind for constant SST with, and without, wind–evaporation dependence.

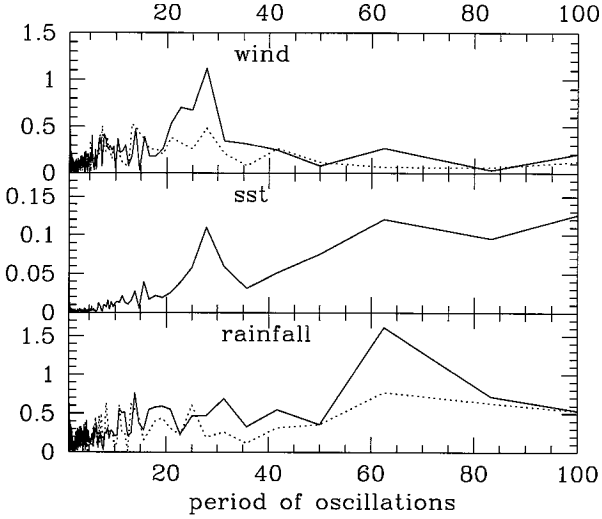

FIG. 12. Spectral analysis of SST, wind, and rainfall for constant SST (dashed line) and modified SST (solid line).

section use the aquaplanet version of the model, with a zonally symmetric SST distribution given by the equation

$$\mathrm{SST} = 29.0 \cos^3\beta + 273.16,$$

where β is a measure of the distance from the equator. This gives the maximum SST equal to 29°C on the equator and minimum 0°C near the poles. The model contains no radiative parameterization, so a Newtonian term is used to relax the atmospheric temperatures to the prescribed vertical distribution. SST is constant in time, except for the narrow equatorial region, within 7°lat distance from the equator, where SST is modified depending on the low-level winds. This SST modification is based on the relationship between equatorial winds and SST changes derived from observations discussed in the previous section. As indicated in Fig. 4, the temperature is assumed to increase in time for small wind velocities, with the maximum of 0.12 K day^{-1} for $u = -3$ m s^{-1}. The SST decrease is equal to 0.13 K day^{-1} for wind velocities between 2 and 10 m s^{-1}. For zonal winds less than -7 m s^{-1} and greater than 12 m s^{-1}, the SST change is equal to zero. The general character of the relationship is similar to that seen in Fig. 4 except for the fact that we have increased slightly the magnitude of cooling relative to the average seen in this figure. The rationale for this increased cooling is based on the fact that the CEPEX 7–14 March event was weaker than the westerly bursts related to the intraseasonal oscillation (as observed during the TOGA-COARE IOP), and SST drops observed during CEPEX were smaller than those occuring during the IOP. Even though the model does not contain a radiative parameterization or the effects of clouds, the asymmetry between SST change for nondisturbed (easterly winds) and disturbed (westerly winds) periods implicitly reflects the effects of SST cooling by shortwave reduction by clouds. Because of the highly simplified nature of our SST equation, a Newtonian damping term is added, with a timescale of 30 days, relaxing the SSTs to the prescribed zonally symmetric state. The timescale for the Newtonian relaxation of SST was determined exerimentally. If the dumping terms are too small, equatorial temperature rises and meridional SST gradient increases. Larger meridional SST gradient causes stronger SST, which in our simple parameterization induces larger SST. Therefore, for the Newtonian dumping we chose the largest timescale that keeps the average equatorial temperature constant.

Results of three model runs are presented here. In the first experiment, the model is run with steady-state SST. In the second, the SST is modified according to the relationship discussed above. In a third experiment we use steady-state SST and, in addition, assume constant wind speed in calculations of latent and sensible heat fluxes to eliminate WISHE modes.

As can be seen from Fig. 10a, in the case of steady SST, the equatorial circulation is dominated by a wave propagating around the globe with a phase speed of about 20 m s^{-1} and low wavenumber perturbations ($s = 1$ and $s = 2$) dominating in the zonal direction. When we neglect the wind–evaporation relationship (Fig. 10b), the propagating wind features are significantly reduced, suggesting that the modes observed in Fig. 10a are a combination of Kelvin and WISHE modes. The spectral analysis of equatorial wind shown in Fig. 11 indicates that WISHE modes, removed by setting the surface wind to a constant, have periods of 20–30 days, which agrees with periods of WISHE modes obtained by Emanuel (1987) or Neelin (1987).

The situation changes if we allow for wind–SST dependence in the equatorial region. The most dramatic change can be observed in rainfall (Fig. 12) where the 40–60 day modes become dominant. As shown in Fig.

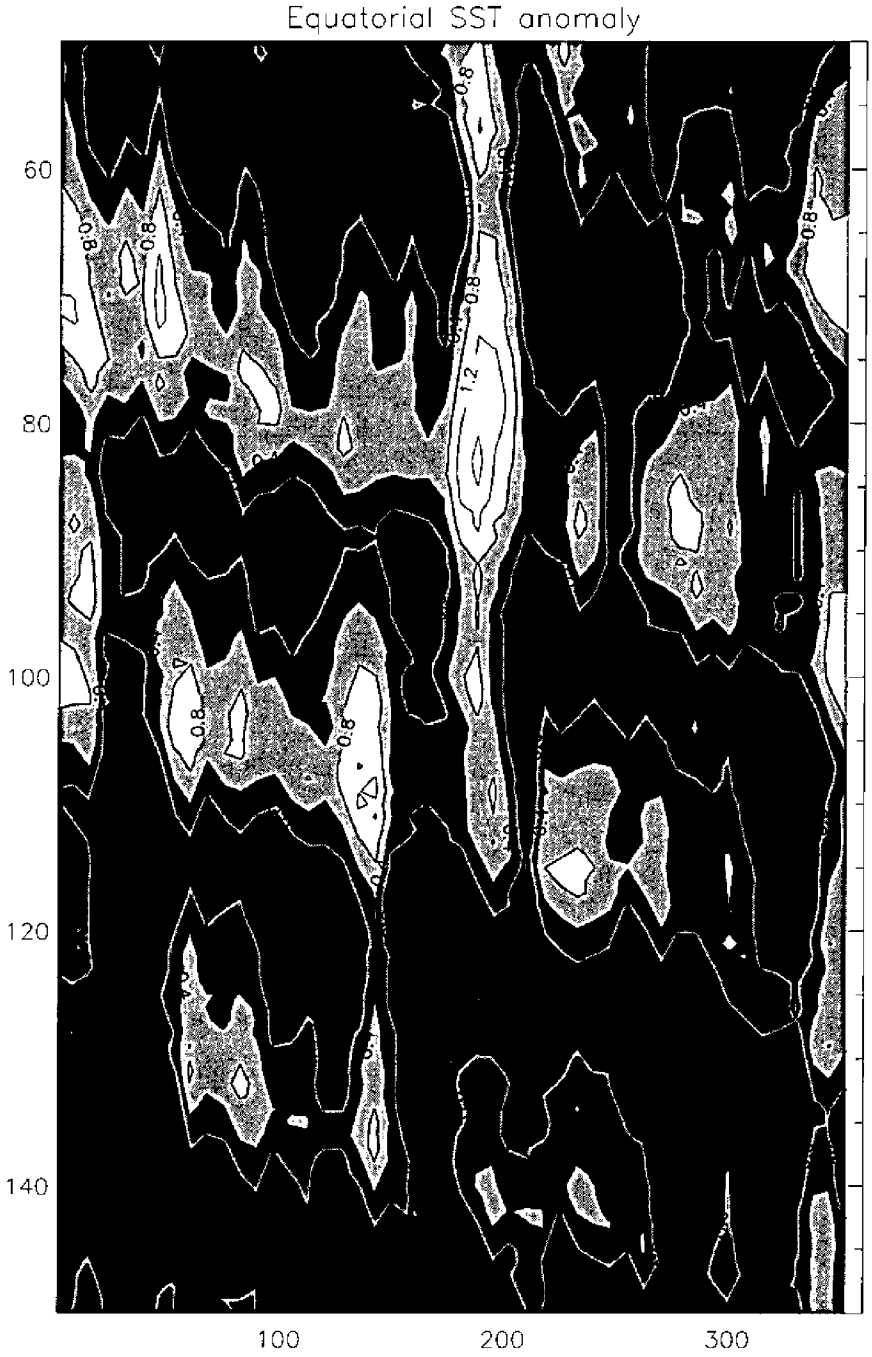

FIG. 13. Longitude–time (in days) diagram of the equatorial SST anomaly (difference from the prescribed steady state for the model run with time-dependent SST, in °C. Contours are labeled every 0.47°C.

10, the wind perturbations become more organized and their phase speed decreases. In the spectral analysis of the equatorial zonal wind (Fig. 12), the amplitude of the mode with a 30-day period increases, which suggests that WISHE modes were amplified by including SST perturbations. In addition, the slower mode, with the period corresponding to a dominant mode in the rainfall, begins to develop.

In the numerical experiments described above, we do not attempt to produce a realistic depiction of intraseasonal oscillations. However, we have been able to show that within the framework of our model, SST modifi-

cations with realistic magnitudes and timescales (Fig. 13) can influence convective development and circulation, leading to amplification of equatorial modes with frequencies similar to those of the observed intraseasonal oscillations.

4. Summary and conclusions

This paper discusses the feedback between SST changes caused by equatorial convection and the dynamics of the intraseasonal oscillation. Using observational results from March 1993 and related TOGA COARE observations (Webster 1994; Serra et al. 1997), we formulate a conceptual model of the interaction between equatorial atmospheric processes and local SST changes. In our conceptual model (ASCII), the sea surface temperature decreases under and west of a convective source. This SST drop is due to the cloud shielding effect, ocean mixing, and evaporative fluxes associated with strong equatorial westerly winds. East of the convective source, in the region of weak winds associated with the convergent region of an easterly propagating Kelvin wave, SST can increase. This zonal SST gradient causes zonal changes in surface moist static energy and provides surface forcing, promoting development of convection in convergent regions. A simple wind–SST change equation based on this conceptual model is used in a simple numerical model to test our hypothesis. The results of calculations presented in this paper suggest that the influence of local SST changes, neglected in most theories of intraseasonal oscillation, provides an important mechanism modifying the oscillation. As shown in our numerical calculations, including this local SST modification can slow down the eastward propagating modes and amplify signals with 40–60 day periods.

Our conceptual model agrees with the observations of Lau and Sui (1997), who found the SST increase related to radiative warming ahead of the convection in TOGA-COARE IFA array. The analysis of the NCEP/NCAR Reanalysis dataset (Sperber et al., 1996) shows a similar pattern of SST anomalies associated with the eastward migrating convection, supporting our conclusions of the coupled nature of intraseasonal oscillations.

It is also worth noting that the effects of SST changes should influence the oscillations of a stationary tropical heat source in the theory of Hu and Randall (1994). They postulate that intraseasonal oscillations are triggered by a time-dependent but stationary heat source. In their model, the convective energy accumulates in the absence of convection because of radiative cooling aloft and increasing moisture above the surface. We postulate that local SST changes associated with convection would operate in phase with this mechanism and make lapse rates even more unstable in nondisturbed regions. On the other hand, the development of convection would lead not only to the low-level drying but also to cooling of the surface temperatures. Including the effects of SST change could greatly influence the period and amplitude of these oscillations. The preliminary results of the coupled one-dimensional model of the MJO (Stevens et al. 1989) indeed show the influence of SST feedback on the behavior of the modeled oscillation.

Acknowledgments. This research was supported by NSF Grant ATM94-13294. Patricia Phoebus was supported by Space and Naval Warfare Systems Command (PMW-175), Program Element 0603207N. Comments of Dr. Kerry Emanuel and anonymous reviewers helped us to clarify our ideas and improve the manuscript. The authors are grateful to Dr. Jim Goerss from the Naval Research Laboratory for his help in producing the NOGAPS analyses and to Dr. William Collins (SIO) for providing the GMS data. Dr. Nicholas Graham's (SIO) help in obtaining and modifying the numerical model used in this paper is appreciated. ECWMF analyzed fields were obtained from NCAR data archive.

REFERENCES

Bi, K., 1995: Variability of the surface layer circulation in the western equatorial Pacific. Ph.D. thesis, University of California, San Diego, 165 pp. [Available from Scripps Institution of Oceanography, La Jolla, CA 92093.]

Brown, R., and C. S. Bretherton, 1995: Tropical wave instabilities: Convective interaction with dynamics using Emanuel convective parameterization. *J. Atmos. Sci.,* **52,** 67–82.

Chang, C. P., 1977: Viscous internal gravity waves and low-frequency oscillations in the tropics. *J. Atmos. Sci.,* **34,** 901–910.

Collins, W. D., F. P. J. Valero, P. J. Flatau, D. Lubin, H. Grassl, and P. Pilevskie, 1996: Radiative effects of convection in the tropical Pacific. *J. Geophys. Res.,* **101,** 14 999–15 012.

Emanuel, K. A., 1987: An air–sea interaction model of intraseasonal oscillations in the tropics. *J. Atmos. Sci.,* **44,** 2324–2340.

——, 1991: A scheme for representing cumulus convection in large-scale models. *J. Atmos. Sci.,* **48,** 2313–2335.

Flatau, M., and P. J. Flatau, 1996: The role of SST feedback in development of equatorial convection. Preprints, *Eighth Conf. on Air and Sea Interaction,* Atlanta, GA, Amer. Meteor. Soc., J124–J127.

Gill, A. E., 1980: Some simple solutions for heat-induced tropical circulation. *Quart. J. Roy. Meteor. Soc.,* **106,** 447–462.

Goerss, J. S., and P. A. Phoebus, 1992: The navy's operational atmospheric analysis. *Wea. Forecasting,* **7,** 232–249.

——, and R. A. Jeffries, 1994: Assimilation of synthetic tropical cyclone observations into the Navy Operational Global Atmospheric Prediction System. *Wea. Forecasting,* **9,** 557–576.

Hogan, T. F., and T. E. Rosmond, 1991: The description of the Navy Operational Global Atmospheric Prediction System's spectral forecast model. *Mon. Wea. Rev.,* **119,** 1786–1815.

Hu, Q., and D. Randall, 1994: Low-frequency oscillations in radiative–convective systems. *J. Atmos. Sci.,* **51,** 1089–1099.

Khain, A., and I. Ginis, 1991: The mutual response of a moving tropical cyclone and the ocean. *Contrib. Atmos. Phys.,* **64,** 125–141.

Kindle, J. C., and P. A. Phoebus, 1995: The ocean response to operational westerly wind bursts during the 1991–1992 El Niño. *J. Geophys. Res.,* **100,** 4893–4920.

Lau, K. M., and L. Peng, 1987: Origin of low-frequency (intraseasonal) oscillations in the tropical atmosphere. I. Basic theory. *J. Atmos. Sci.,* **44,** 950–972.

——, and C. Sui, 1997: Mechanism for short-term sea surface temperature regulation: Observations during TOGA COARE. *J. Climate,* **10,** 465–472.

——, L. Peng, C. H. Sui, and T. Nakazawa, 1989: Dynamics of super cloud clusters, westerly wind bursts, 30–60 day oscillations and ENSO: An unified view. *J. Meteor. Soc. Japan,* **67,** 205–219.

Li, T., and B. Wang, 1994: The influence of sea surface temperature on the tropical intraseasonal oscillation: A numerical study. *Mon. Wea. Rev.,* **122,** 2349–2362.

Lin, K., and R. H. Johnson, 1996: Kinematic and thermodynamic characteristics of the flow over the western Pacific warm pool during TOGA COARE. *J. Atmos. Sci.,* **53,** 695–715.

Madden, R. A., and P. R. Julian, 1971: Detection of a 40–50 day oscillation in the zonal wind in the tropical Pacific. *J. Atmos. Sci.,* **28,** 702–708.

Nakazawa, T., 1988: Tropical super clusters within intraseasonal variations over the western Pacific. *J. Meteor. Soc. Japan,* **66,** 823–839.

——, 1995: Intraseasonal oscillations during the TOGA-COARE IOP. *J. Meteor. Soc. Japan,* **73,** 305–319.

Neelin, J. D., I. M. Held, and K. H. Cook, 1987: Evaporation–wind feedback and low-frequency variability in the tropical atmosphere. *J. Atmos. Sci.,* **44,** 2341–2348.

Ralph, E. A., K. Bi, K. K. Niiler, and Y. Penhoat, 1997: A Lagrangian description of the western equatorial Pacific response to the wind burst of December 1992: Heat advection in the warm pool. *J. Climate,* **10,** 1706–1721.

Ramanathan, V., and W. Collins, 1991: Thermodynamic regulation of ocean warming by cirrus clouds deduced from observations of the 1987 El Niño. *Nature,* **351,** 27–32.

Serra, Y., D. P. Rogers, D. E. Hagan, C. A. Friehe, R. L. Grossman, R. A. Weller, and S. Anderson, 1997: The atmospheric boundary layer over the central and western ocean observed during TOGA-COARE and CEPEX. *J. Geophys. Res.*, in press.

Sperber, K., J. Slingo, P. M. Inness, and W. K.-M. Lau, 1996: On the maintenance and initiation of the intraseasonal oscillations in the NCEP/NCAR reanalysis and the GLA and UKMO AMIP simulations. PCMDI Rep. 36, 60 pp. [Available from UC, Lawrence Livermore National Laboratory, Livermore, CA 94550.]

Stevens, D. E., Q. Hu, G. L. Stephens, and D. A. Randall, 1989: The hydrological cycle of the intraseasonal oscillation. *Proc. Western Pacific International Meeting and Workshop on TOGA-COARE,* Noumea, New Caledonia, 485–492.

Webster, P., 1994: The role of hydrological processes in ocean–atmosphere interactions. *Rev. Geophys.,* **32,** 427–476.

——, A. C. Clayson, and J. A. Curry, 1996: Clouds, radiation, and the diurnal cycle of the sea surface temperature in the tropical western Pacific. *J. Climate,* **9,** 1712–1730.

Yu, J., and J. D. Neelin, 1994: Models of tropical variability under convective adjustment and the Madden–Julian oscillation. Part II: Numerical results. *J. Atmos. Sci.,* **51,** 1895–1914.